FEATURE ARTICLE

Time-Resolved Circular Dichroism Spectroscopy: Experiment, Theory, and Applications to Biological Systems

James W. Lewis, Robert A. Goldbeck, David S. Kliger,*

Department of Chemistry and Biochemistry, University of California at Santa Cruz, Santa Cruz, California 95064

Xiaoliang Xie, Robert C. Dunn, and John D. Simon*

Department of Chemistry, University of California at San Diego, La Jolla, California 92037-0341
(Received: February 12, 1992)

Recent advances have made it possible to improve the time resolution of natural and magnetically induced circular dichroism spectral measurements from the millisecond to the nanosecond and picosecond time regimes. These techniques are described along with several applications which demonstrate the utility of these measurements. Specific applications to studies of heme protein structural changes following ligand photodissociation and of intermediates of bacterial photosynthetic reaction centers are presented which demonstrate the ability of these techniques to provide new information about the structural dynamics and electronic states of reaction intermediates.

I. Introduction

Relationships between the structure, function, and reactivity of biological molecules are a topic of great experimental interest. Depending on the complexity of the chemical process, important structural changes in reacting molecules can occur over a large range of time scales. Upon the absorption of visible light, for example, the retinal chromophore in rhodopsin[1] and bacteriorhodopsin[2] isomerizes in less than a picosecond. Motions of amino acid side chains in proteins generally occur on the picosecond to nanosecond time scale,[3] and large-scale structural changes within the interior of a protein can require times ranging from nanoseconds to seconds.[4] In particular, the quaternary structure change associated with the R → T transition in photodissociated hemoglobin takes microseconds.[5] In understanding the relationships between the structure and function of biological systems, it is important to determine the time scales associated with the particular molecular motions that lead to chemical reactivity.

Many experimental techniques have been developed to probe the time scales of structural changes. Experimental probes include various steady-state spectroscopies in which line widths are used to gain information. In recent years, significant insights into protein motions have resulted from the development of multidimensional nuclear magnetic resonance (NMR) techniques.[6] In addition, direct time-resolved spectroscopies utilizing fast mixing or equilibrium perturbation have been successful in observing events on the microsecond time scale. Recent advances in laser technology have opened up the ultrafast region extending into the femtosecond domain.[7]

In 1953, Weber[8] demonstrated that time-resolved polarized emission could be used to determine rotational time scales of large biomolecules. With further advances in detection electronics and short light pulse generation, emission spectroscopy is now capable of resolving motions of chromophores well into the subpicosecond time scale.[9] Only motions which occur during the excited-state lifetime of the chromophore can be studied in this way. This generally limits the ability of this technique to motions that take place faster than a few nanoseconds. Transient absorption and linear dichroism spectroscopy are not limited in this manner and have been used to probe intermediate states in many photobiological processes.[10] Absorption techniques that probe optical and vibrational transitions with time resolutions as fast as ~0.1 ps have significantly advanced our understanding of many biological processes.[2a,11] Similar to emission-based techniques, the underlying physics of absorption spectroscopies render them sensitive to only local motions of particular chromophores in the protein structure that absorbs the incident light. Clearly what is needed is a complementary time-resolved technique sensitive to the global rearrangements that biomolecules undergo.

The related techniques of optical rotation and circular dichroism (CD) spectroscopy have been extensively used to investigate global protein structure.[12] The discovery of chiral secondary structures in many important classes of biomolecules has placed these methods in the forefront of secondary structure studies of DNA, RNA, and proteins. These techniques are useful for quantifying the composition of secondary structures of biomolecules in solution. In the past few years, structural studies of biological molecules have advanced beyond the questions of static equilibrium structures to the issues of the nature and time scales of their dynamics. In many systems, this involves studying the dynamics by which changes in the secondary structure occur. While such changes are difficult to detect using conventional time-resolved absorption and emission techniques, it is clear that these should, in principle, be measurable by time-resolved circular dichroism (TRCD) spectroscopy or time-dependent optical rotation. The need to quantify the dynamics of structure changes in biomolecules prompted our efforts to develop experimental techniques for measuring TRCD spectra over the large range of time scales characteristic of these important processes.

From a purely theoretical standpoint there is no reason to prefer CD over optical rotation. The two measurements are related by the Kramers-Kronig transform and therefore provide the same information. It is from a practical standpoint that CD is preferred. This is easily understood by examining how the two measurements are related. Circular dichroism is an absorptive property of the system, quantified by the difference in molar extinction coefficient, $\Delta\epsilon$, for left, ϵ_L, and right, ϵ_R, circularly polarized light:[13]

*To whom correspondence should be addressed.

0022-3654/92/2096-5243$03.00/0 © 1992 American Chemical Society

$$\Delta\epsilon = \epsilon_L - \epsilon_R \quad (1)$$

This quantity is nonzero only in the spectral regions in which the molecule under study has optical transitions. On the other hand, optical rotation is a dispersive measurement. Thus, an accurate measurement requires studying the molecule over the complete spectrum. Generally, this is not possible and experiments are usually confined to a relatively small wavelength range. Furthermore, optical rotation measurements combine information about many electronic transitions while CD depends only on the particular transition which is responsible for the observed absorbance. For these reasons CD is preferred over optical rotation for studying structural dynamics in biomolecules.

II. Methods

Steady-State Techniques. Early measurements of CD by Cotton[14] took advantage of the fortuitous discovery of a chromium tartrate complex with an extraordinarily high $\Delta\epsilon$ relative to ϵ (1 part in ~20). This enabled detection of CD directly by the eye using relatively unsophisticated methods. These consisted essentially of passing beams of left and right circularly polarized light side by side through a liquid sample and comparing the transmitted intensities with one another in the same field of view. The relative size of the $\Delta\epsilon$ of the chromium tartrate complex overwhelmed potential artifacts (which include the slight differential sensitivity of the eye to left and right circularly polarized light). While more sophisticated (and sensitive) techniques were already available when Cotton made his measurement, the simplicity of his optical method made the result convincing. Previously, CD in crystals had been reported by Haidinger,[15] but the potential artifacts of measurements in anisotropic media using a more complex optical method made the result harder to interpret in strictly molecular terms.

In the early part of the 20th century some progress was made in studying the CD of solutions using a variety of ingenious optical methods, often based on photographic detection.[16] Some of these methods took advantage of the fact that CD produces ellipticity in a beam of linearly polarized light while traversing a sample (a fact also demonstrated by Cotton). By analyzing the ellipticity of the emerging light, one could determine the CD of samples, assuming that no other source of ellipticity was present.

The development of photoelectric detectors and associated improvements in electronic detection returned interest to a variation of Cotton's difference method. Instead of comparing the intensity of two beams of circularly polarized light which simultaneously traversed the sample, the polarization of a single beam was modulated between right and left circular forms before passing through the sample. Circular dichroism then caused the detected intensity to be modulated at the frequency at which the polarization was switched. This method had important potential advantages in reducing noise due to intensity fluctuations in the light source used for the measurements.

Modulation methods dramatically improved the signal-to-noise ratio of CD measurements as better polarization modulators were found. In practice, polarization modulators consisted of devices which alternated between +1/4 and −1/4 wave of retardation of a linearly polarized probe beam. When a probe beam, linearly polarized at 45° to the retardation axis, is passed through such a device, the emerging beam alternates between right and left circular polarizations. To provide the required variable retarder, first the Pockels cell[17] and then the photoelastic modulator[18] were introduced, offering electronic control over polarization with steadily reduced levels of polarization artifacts. Unfortunately, these improvements also progressively limited the flexibility of the method in the time domain. Since modulation methods compare successive intensities of right and left circularly polarized light, their time resolution was limited to several periods of the modulation frequency. For photoelastic modulators this produced a limit in the millisecond region. Improvements in time resolution by increasing the frequency of photoelastic modulators did not seem promising because of the resonant character of such devices. At the beginning of the past decade this impasse limited the absolute time resolution of CD measurement. Even approaching it was very difficult, and only limited experiments had been conducted on kinetic changes in proteins produced under stop-flow conditions.

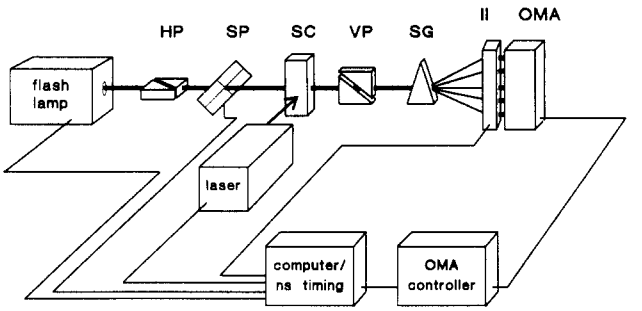

Figure 1. Experimental apparatus for measuring ellipsometric CD signals with nanosecond resolution. An electronic gate pulse from a nanosecond pulse/delay generator determines the time resolution of detection by modulating the gain of the image intensifier (II) stage of an optical multichannel analyzer (OMA). A computer synchronized with the timing pulse generator collects data from the OMA controller and reverses the orientation of the strain plate (SP) between flashes. A Glan–Taylor prism (HP) horizontally polarizes a broad-band pulse from the flashlamp. The linearly polarized beam acquires slightly elliptical polarization from the ca. 1° retardance of the strain plate before it enters the sample cell (SC). The strain plate is a fused silica plate compressed along an axis oriented at ±45° from horizontal (measured counterclockwise looking toward the source), producing left and right elliptically polarized light, respectively. A vertical prism polarizer (VP) analyzes the ellipticity of the transmitted probe beam. A spectrograph (SG) disperses the beam to the image intensifier at its output plane. The difference signal between left and right elliptically polarized probe light is proportional to the CD of the sample.

The usual problem to be overcome in measuring CD is that $\Delta\epsilon$ is very small compared to the extinction coefficients themselves, often as little as 1 part in 10^4–10^6. Measuring such small signals with high time resolution raises shot noise issues which distinctly favor a dispersive measurement like optical rotation over an absorptive one like CD. Further, the probe intensities required to overcome shot noise limits pose a definite threat to the photolabile molecules which are often the subjects of rapid, time-resolved experiments. Considering these difficulties, it is important to stress that the interpretation of CD measurements in terms of structural changes is more tractable than that of optical rotation. There are many excellent reviews on the theoretical principles underlying the shapes and magnitudes of CD spectra.[19]

Milli- and Microsecond Time-Resolved Techniques. To address questions about protein dynamics of current interest, faster methods were needed to probe the time scales on which secondary structure changes occur, but these methods still had to be sensitive enough to detect the very small changes involved. Initial attempts to measure CD with improved time resolution used perturbation techniques such as stopped flow,[20] temperature jump,[21a,b] pressure jump,[21c] and flash photolysis[21d] measurements coupled with standard CD instrumentation. This allowed the measurement of CD changes with a time resolution on the order of milliseconds. Circularly polarized luminescence (CPL) techniques[22] have also been developed which make it possible to make CD measurements with improved sensitivity.

Nanosecond Circular Dichroism. As discussed above, modern methods of measuring CD have employed photoelastic modulators to rapidly modulate the polarization of the measuring light beam. This is very important for high signal-to-noise measurements as CD is a small effect, and signal averaging is important for its direct measurement. Unfortunately, standard methods for measuring CD are not effective for measurements with nanosecond time resolution. Photoelastic modulators are generally limited to the 100-kHz range, limiting time resolution of CD measurements to milliseconds. Synchronizing such modulators to nanosecond pulsed lasers is impractical as such lasers have relatively low repetition rates. Thus, direct measurements of CD on a nanosecond time scale are impractical. Instead, an ellipsometric method for

measuring CD has been developed.[23]

As shown in Figure 1, the ellipsometric CD measurements can be made with an instrument that is essentially a modified nanosecond laser photolysis system. Such a photolysis system simply involves a pump laser to initiate reactions of interest, a probe light source to monitor changes in sample absorption, and a detection system to record probe beam intensity changes as a function of time. For CD measurements one measures changes in polarization characteristics (rather than intensity) of the probe beam with time. This is done in the following way. First, the probe beam is passed through a linear polarizer. The resulting linearly polarized beam is then passed through a fused silica plate to which a mechanical strain has been applied along an axis oriented at ±45°. This produces a birefringent optical element which converts the linearly polarized light to highly eccentric elliptically polarized light. (Applying enough strain to produce 1° of retardance produces elliptically polarized light with major axis intensity 10^4 times the minor axis intensity.) When this elliptically polarized probe beam passes through a circularly dichroic sample, the polarization ellipticity changes. This occurs because elliptically polarized light can be decomposed into unequal amplitude circularly polarized components. As the circular polarization components become more unequal, the polarization ellipse becomes fatter. Thus, since a circular dichroic sample will change the relative amplitudes of right and left circularly polarized components, it will increase or decrease the ellipticity of the probe beam, depending on the sign of the CD and the handedness of the elliptically polarized probe beam. Since the probe beam ellipticity is initially highly eccentric, the change in ellipticity can readily be determined by measuring the change in minor axis intensity. This is accomplished by passing the probe beam through a linear polarizer oriented to pass only light along the minor polarization axis. By measuring these changes for both left and right elliptically polarized probe beams, it is possible to determine both the sign and magnitude of the CD. Furthermore, the method is quite sensitive. A CD signal of 1 part in 10^4 will produce a change in the measured ellipticity of 1 part in 10. This sensitivity makes it possible to measure CD spectra with nanosecond time resolution.

Time-resolved magnetic CD can also be measured with nanosecond time resolution with two modifications to the above technique.[23e] The first is to apply a magnetic field to the sample to induce a CD in the sample. The second modification is needed because the magnetic field, in addition to inducing CD, causes a rotation of the polarization axis of the probe beam due to Faraday rotation (which results from cell windows and solvent as well as the molecules under study and can thus be a large effect). To compensate for this Faraday rotation, an optically rotatory element (typically a sugar solution) is placed between the sample and the analyzing polarizer to rotate the probe beam polarization axis to its original orientation. Another complication in measuring MCD spectra by this technique is that many samples will exhibit both MCD and CD. Fortunately, CD and MCD signals are easily separated. The sign of an MCD signal depends on the orientation of the applied magnetic field while the CD signal is independent of magnetic field. Thus, it is straightforward to measure CD signals with opposite magnetic field orientations and sum the two signals to determine the pure CD spectrum or subtract the two signals to determine the pure MCD spectrum.

Picosecond Circular Dichroism. In principle, the experimental approach described in the above section could be modified to enable picosecond CD spectroscopy. In such an approach, the probe light would need to be derived from a picosecond white light continuum. This approach presents some technical problems including intensity instability, polarization scrambling, and tunability limitations associated with continuum generation. Although all of these problems should in principle be solvable, with the development of reliable high repetition rate tunable picosecond lasers, an alternative approach for recording transient CD data appeared to be more attractive.

The experimental apparatus used to collect CD spectra with picosecond resolution is shown in Figure 2.[24,25] A frequency-doubled acoustically mode-locked and Q-switched Nd:YAG laser synchronously pumps two electro-optically cavity dumped dye lasers at a repetition rate of 1.0 kHz. The outputs of the two dye lasers serve as the pump and probe light pulses.[25] The dye lasers can be tuned from 560 to 950 nm, with pulse energies ranging from 1 to 10 μJ and a pulse width of ~50 ps. In addition, by frequency doubling the dye laser, probe light pulses can also be generated from 280 to 475 nm. The output from the Nd:YAG oscillator can also be frequency tripled to 355 nm and used to synchronously pump a dye laser producing microjoule pulses in the spectral region from 375 to 570 nm. These light pulses can be frequency doubled to generate probe pulses in the ultraviolet region.

The collection of transient CD data is a modification of the standard pump–probe absorption optical arrangement. The pump laser pulses travel down a variable delay line, pass through a depolarizer and spinning half-wave plate, and are focused into the sample. Without the depolarizer and spinning half-wave plate, the photoselection caused by a polarized pump laser pulse gives rise to linear dichroism signals that make detection of the transient CD signal impossible.[26]

The probe laser pulses pass through a polarizer followed by a photoelastic modulator. The modulator controls the firing of the Q-switch in the Nd:YAG oscillator such that successive probe laser pulses pass through the modulator when $+\lambda/4$ and $-\lambda/4$ voltage is being applied. These pulses are focused through the region of the sample excited by the pump laser and detected by a head-on photomultiplier tube (PMT). The voltage output of the PMT is gated by a track-and-hold circuit and fed into a lock-in amplifier that is referenced to the polarization modulation frequency. Comparing the output of the lock-in amplifier to the dc signal from the track-and-hold circuit provides a direct measure of the sample CD. The experiment is controlled by a MAC-II computer using LabView. In order to ensure the linear response of the PMT, a variable neutral density filter is placed before the PMT to control the intensity of the light that is sent to the detector. The variable neutral density filter is automatically adjusted by a feedback-servo system so that the integrated voltage received by the track-and-hold circuit from the amplified PMT output is maintained constant for a constant bias voltage. This enables accurate measurements of the CD signals to be made when large changes in optical density occur in the sample.

Kinetics are recorded by scanning the delay line in the pump laser optical path. Detailed accounts of the modifications made to this apparatus to enable recording transient spectra[27] as well as picosecond MCD dynamics[28] can be found elsewhere.

III. Optical Artifacts and Their Cures

CD measurements are sensitive to interference from other optical properties, such as circular birefringence (CB), linear birefringence (LB), or linear dichroism (LD), that may be present in the sample or optical train. This sensitivity depends on the method employed. Most generally, CD is measured by probing the sample with a light beam of well-defined transverse polarization and detecting the transmitted intensity. Specific CD methods are distinguished by the type of polarization employed and whether total transmitted intensity (absorptive method) or polarization state of the transmitted beam (ellipsometric method) is measured. (The latter approach usually requires placement of an analyzing polarizer after the CD sample.) Ellipticity, defined here as the ratio of minor to major axis electric field amplitude, characterizes the probe beam polarization. The generation of nonzero elliptical polarization from horizontal linear polarization by a modulating linear retardance, δ, oriented at 45° from horizontal is illustrated in Figure 3 for two cases, $\delta = \pi/2$ and $0 < \delta \ll 1$. The amount of ellipticity induced is given by eq 2.

$$\xi = ((1 - \cos\delta)/(1 + \cos\delta))^{1/2} \quad (2)$$

Probe Ellipticity and Signal/Noise. The case of $\delta = \pi/2$ generates circularly polarized light ($\xi = 1$), the polarization used in conventional CD instruments and in the picosecond TRCD apparatus because it gives the maximum signal to noise in an absorptive measurement of CD. The ellipsometric method used

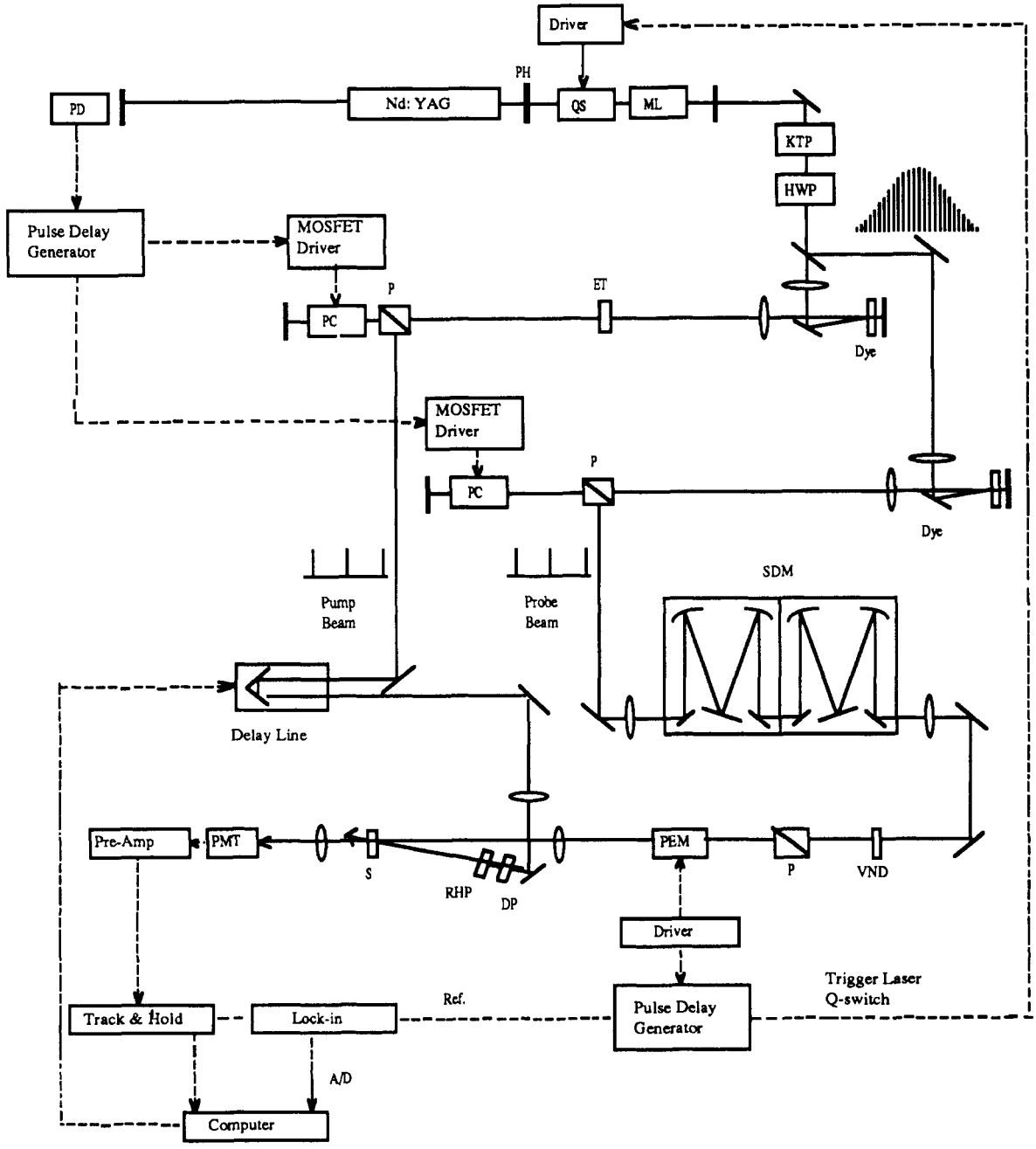

Figure 2. Transient picosecond circular dichroism spectrometer. Abbreviations used: PD, photodiode; ML, acousto-optic mode locker; QS, acousto-optic Q-switch; PH, pinhole; KTP, $KTiOPO_4$ nonlinear crystal; PC, electro-optic Pockels cell; ET, etalon; P, polarizer; PEM, photoelastic modulator; RHP, rotating half-wave plate; DP, depolarizer; SDM, subtractive double monochromator; VND, variable neutral density filter; S, sample; PMT, photomultiplier tube. The mode-locked and Q-switched YAG synchronously pumps two dye lasers. These provide the pump and probe picosecond pulses. The pump beam is depolarized, with any residual polarization being modulated by a rotating half-wave plate. The probe beam is polarization modulated using a photoelastic modulator. The detection is referenced to the polarization modulation rate, providing a direct measure of the sample CD. Time resolution is achieved by varying the relative path lengths traveled by the pump and probe laser pulses.

in the nanosecond TRCD apparatus, on the other hand, is best carried out with nearly linear polarization ($\xi = \delta/2 \ll 1$). Perfectly linear polarization ($\xi = 0$) is not suitable because of interference from circular birefringence intrinsic to the CD sample.[29] The modulating retardance must be much larger than intrinsic CB but still small enough to give amplification of the signal relative to instrumental noise. Instrumental noise, such as drift in lamp intensity, is taken to be proportional to lamp intensity and is distinguished from photon shot noise, which increases as the root of the intensity. The signal (for $CDz \ll 1$, in the absence of artifacts) is given by

$$S = (I_R - I_L)/(I_R + I_L) = \mathrm{CD} \sin \delta\, (T_x + 1)z/(\sin^2 \delta/2 + T_x \cos^2 \delta/2) \quad (3)$$

where $CD = 0.575c\,(\epsilon_L - \epsilon_R)$ is the CD (per unit path length), z is the path length (cm), and c is the concentration (moles/liter). $T_x = 1$ defines an absorptive CD measurement and $T_x = 0$ an ellipsometric measurement. Since S is a relative signal, we consider its ratio to relative noise, N. For instrumental noise, set $N = f$ where f is a constant between 0 and 1. The signal-to-noise ratio in this case is given by

$$S/N = \mathrm{CD} \sin \delta(T_x + 1)z/(f(\sin^2 \delta/2 + T_x \cos^2 \delta/2)) \quad (4)$$

For an absorptive measurement, S/N reaches a maximum value of $2CDz/f$ at $\delta = \pi/2$. For an ellipsometric measurement, this ratio is $2CDz/(f \tan \delta/2)$ which increases as δ approaches a lower limit set by artifactual and other considerations. The ratio of S/N for ellipsometric ($\delta \ll 1$) vs absorptive measurements ($\xi = 1$) is $2/\delta$, indicating a S/N advantage for the ellipsometric method.[30] In practice, $\delta = 10^{-2}$ rad is a typical value that avoids intrinsic CB and other artifacts while amplifying signal/instrument noise relative to an absorptive measurement by roughly 10^2. On the

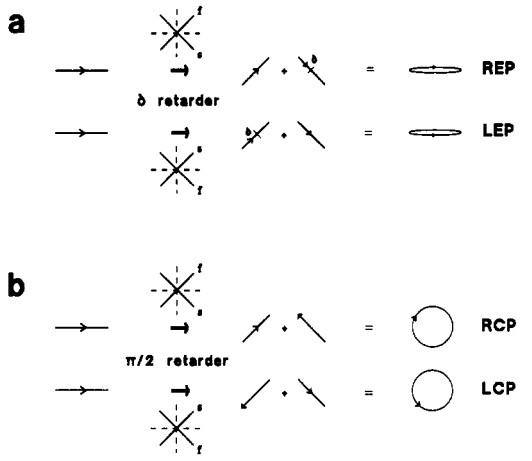

Figure 3. (a) A retardance of $\delta \ll 1$ converts horizontally polarized light to slightly elliptically polarized light, ellipticity $\approx \delta/2$. When the retarder is oriented with its slow axis 45° clockwise from the horizontal (top example), the linear component of the light parallel to this axis receives a slight phase delay δ relative to the perpendicular component (crossbar shows perpendicular phase). This retarder orientation makes right elliptically polarized (REP) light. A compressed fused silica plate is the retarder in ellipsometric TRCD. The plate is rotated by 180° around vertical to produce LEP light. (b) A retardance of $\pi/2$ converts horizontally polarized light to circularly polarized light, ellipticity = 1. A $\pi/2$ retarder (quarter-wave plate) with its slow axis oriented 45° clockwise from horizontal produces tight circularly polarized (RCP) light by phase delaying the parallel linear component of the light from the perpendicular component. In conventional and picosecond absorptive CD measurements, quarter-wave retardance is provided by a fused silica block that is compressed and decompressed by a driver in acoustic resonance with the retarder in order to produce alternating RCP and LCP light.

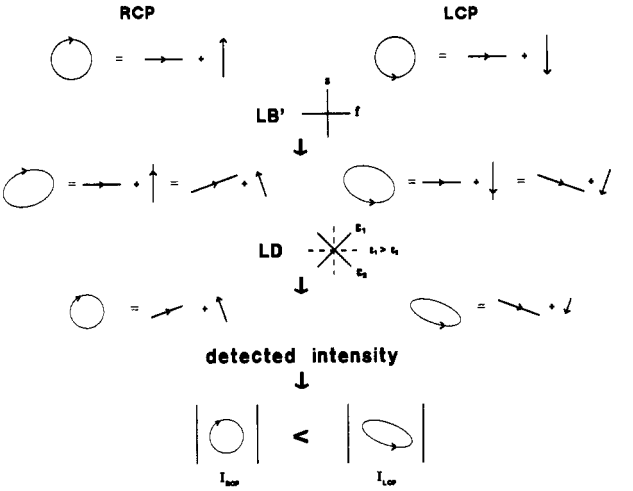

Figure 4. Coupling of pump-induced sample LD with extraneous LB′ to produce an artifactual CD signal is illustrated for an absorptive CD measurement. (A similar mechanism also couples LD and LB′ in ellipsometric measurements.) The worst case LB′ is shown, LB′ oriented 45° askew from the LD. Phase delay induced in the vertical light component by LB′ results in elliptical polarization with its major axis rotated away from the horizontal. The direction of rotation depends on the circular handedness of the incident light. A measurement of total intensity at this point would show no difference between right- and left-handed polarizations. However, the LD shown intervening between LB′ and the detector preferentially passes left-handed light, in this case, because the major axis of the left-handed ellipse is partially aligned with the LD axis of greatest transmission.

other hand, the signal/photon shot noise ratios of the ellipsometric and absorptive methods are generally comparable. This can be seen by setting (relative) shot noise $N' = [I(\sin^2 \delta/2 + T_x \cos^2 \delta/2)]^{-1/2}$, where I is the intensity transmitted through the sample. In this case, signal to noise is given by

$$S/N = CDz \sin \delta(T_x + 1)I^{1/2}(\sin^2 \delta/2 + T_x \cos^2 \delta/2)^{-1/2} \quad (5)$$

For an absorptive measurement, this reduces to $2CDzI^{1/2} \sin \delta$. As expected, this is maximized at $\delta = \pi/2$ and is proportional to the root of intensity. For an ellipsometric measurement, this becomes $2CDzI^{1/2} \cos \delta/2$, which reaches the same maximum value at small values of δ as an absorptive measurement at $\delta = \pi/2$ (assuming that I is constant between methods, i.e., the same light throughput as measured after the sample). Thus, the absorptive and ellipsometric CD techniques have identical shot noise figures when used with the optimum probe ellipticities.

Circular Birefringence. The effect of CB must be considered in evaluating CD methods because of the basic physical connection between the two optical effects. This connection is summarized in the Kramers–Kronig relation, which shows that any CD active absorption band is accompanied by an intrinsic CB in the spectral region near that band.[31] It is well-known for conventional CD measurements that CB does not contribute in first order to the measured signal, but this may not be as evident for the ellipsometric method discussed here. Like conventional CD, the ellipsometric method measures a difference signal between oppositely handed polarizations, normalized to the sum of intensities. Because the effect of CB, rotation of the polarization ellipse, is identical for both right- and left-handed polarizations, it cancels from the difference. Although the intrinsic CB does enter in second order into the normalizing factor, its effect can always be made negligible by using a sufficiently large value of δ. An important exception to this consideration occurs in magnetic CD measurements, where the magnetically induced CB of the transparent cell windows and solvent can be very large. In this case, it is straightforward to compensate for rotation of the polarization ellipse with an opposite rotation from an optically active substance transparent in the spectral region of interest, e.g., an optically resolved sugar solution for measurements in the near-UV/visible region.[23e] Because CD and CB are commuting optical effects, i.e., their order in the optical train is immaterial (neglecting any intervening LB or LD), this leaves the measurement of CD unaffected.

Linear Dichroism and Birefringence. It is well-known that absorptive CD methods are not appreciably affected by linear dichroism or birefringence acting alone but that LD in the sample can couple with strain birefringence (LB′) in the optics before the sample and distort the measured CD signal. A generalization of previous Jones matrix analyses for external strain to a sample exhibiting intrinsic CD, CB, LB, and LD shows that, for small LD, LB′, and CD, the size of the LD, LB′ coupling relative to the CD of interest in both absorptive and ellipsometric measurements is given by

$$(\text{LD, LB}' \text{ coupling artifact})/(\text{CD signal}) = 2(\text{LD})(\text{LB}') \sin (2\rho - 2\theta)/\Delta\epsilon \quad (6)$$

where $\Delta\epsilon = \epsilon_L - \epsilon_R$, LD $= \epsilon_x - \epsilon_y$, LB′ is the stray retardance in radians, ρ is the angle of the fast LB′ axis relative to horizontal, and θ is the angle of the LD x axis relative to horizontal.[26,32] This coupling vanishes when the LD and LB axes are aligned and is maximized when the axes are 45° askew, explaining why LD and LB intrinsic to the sample typically do not couple. A worst case example of LD, LB′ coupling is illustrated in Figure 4 for $\rho = 0$ and $\theta = 45°$. In this case, the effect of LB′ on circularly polarized light is to lower the ellipticity from a value of one and create an ellipse with its major axis oriented at ±45°, the sign of the angle depending on the circular handedness. Alignment of the major elliptical axis along the maximum or minimum LD transmission axis results in a different total absorption of right- and left-handed polarized light, i.e., an artifactual signal.

Whereas isotropic samples, e.g., solutions, cannot exhibit LD or LB, excitation with a linearly polarized laser can remove isotropy through photoselection. Because photoselectively induced LD can be quite large, its coupling with the modest amounts of stray strain (time-independent retardance of 1–10°) typically found in CD cells and polarization modulators can be comparable to the time-resolved CD being measured. Such photoselection artifacts are particularly pernicious for time-resolved CD measurements because their spectral localization and time dependence

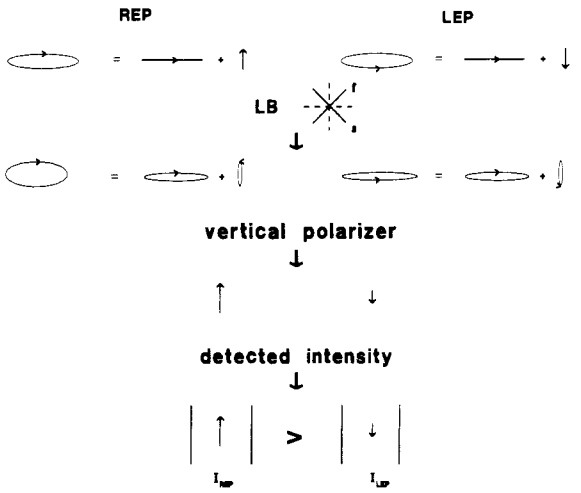

Figure 5. LB with its axis askew from the elliptical polarization axes can produce an artifactual signal in an ellipsometric CD measurement. (This effect is analogous to the LB′, LD coupling shown in Figure 4 with LD replaced by the vertical polarizer.) LB acts on the major linear component present in the incident elliptically polarized light to produce, for the LB orientation shown, a major component of right elliptically polarized (REP) character. This augments the extent of REP, and thus the vertical amplitude, of the incident REP light and decreases the vertical amplitude in the case of incident left elliptically polarized (LEP) light.

can mimic the signal of interest. Random rotational motion eventually restores isotropy to dissolved samples on a time scale that depends on temperature, solvent viscosity, and solute size and shape. Typical reorientation time scales for solutions at ambient temperature range from picoseconds for small molecule solutes to nanoseconds for biopolymers and on to milliseconds and higher for organelle-like biological samples. The effects of such pump-induced artifacts must be considered and corrected for in TRCD studies of proteins and other biopolymers on nanosecond and faster time scales. Although an obvious solution is to use a depolarized pump source, in practice it is very difficult to effectively depolarize a laser pulse, i.e., randomize polarization over the spatial or temporal extent of the pulse. The artifact reduction strategy used in the picosecond TRCD apparatus exploits the sinusoidal dependence on orientation angle displayed above.[25a,26] A half-wave plate placed in the actinic laser beam is rotated at a frequency (3.5 Hz) that is much lower than the probe modulation frequency (500 Hz), modulating the orientation of the pump-induced LD relative to the static LB. The low-frequency modulated LD, LB′ coupling signal is easily distinguished by a lock-in amplifier from the true CD signal and averaged to zero using a time constant (3–10 s) much longer than the half-wave plate rotation period.

In addition to the LD, LB′ coupling found in absorptive CD methods, the ellipsometric method is also sensitive to the effect of LB in first order, i.e., acting alone,[33,34] as illustrated in Figure 5. The ratio of the LB signal to the CD signal of interest is given by

$$(\text{LB artifact})/(\text{CD signal}) = \text{LB} \sin 2\theta/\text{CD} \qquad (7)$$

where $\text{LB} = \pi(\eta_y - \eta_x)/\lambda$ is the retardance of the sample in rad/cm. A similar expression also holds for external sources of strain birefringence. This means that the nanosecond TRCD apparatus has a greater sensitivity to linear birefringence artifacts than instruments that use an absorptive method. This puts stricter limits on the amount of strain birefringence that can be tolerated in cell windows. In general, stray birefringence must be kept small relative to the strain plate retardance, which is on the order of 1°. Although proper alignment of the window strain axis can minimize the size of the signal offset produced by LB′, excessive values of LB′ will also give a diminuation of signal size that rolls off slowly at higher wavelengths. More important to the accuracy of ellipsometric TRCD measurements is the sensitivity to pump-induced LB artifacts. Because of their CD-like spectral shape, these must be kept small compared to CD. In principle, the rotating half-wave plate technique used in picosecond TRCD could also be used to average the sin 2θ dependence of the LB signal to zero. However, the LB signal can be much larger than LD, LB′ coupling. This fact, along with the much lower repetition rate of the nanosecond apparatus, means that impractically long averaging times would often be required. Instead, strategies that align the pump and probe polarizations such that sin 2θ vanishes have been found to be effective for collinear or quasi-collinear excitation geometries.[32] If 90° excitation geometry can be used, a more effective extension of this approach is to align the actinic polarization vector with the path of the probe beam. From the perspective of the probe beam, alignment of pump polarization with the probe propagation vector gives effectively isotropic excitation of the sample that is particularly stable with respect to small misalignments of beam propagation and polarization vectors. Finally, it should be pointed out that the low light levels transmitted by the quasi-crossed polarizers make this method more vulnerable to interference from light scattering and emission than absorptive measurements. Since the probe light transmitted is proportional to $\sin^2 \xi$, this consideration may set a lower limit on the value of ξ used.

To summarize the issue of TRCD artifacts, pump-induced polarization artifacts become increasingly important with shorter time resolution. The precise nature of the artifacts and their remedies depends on the CD method employed. The nanosecond TRCD apparatus uses a quasi-null ellipsometric method ($\xi \ll 1$) that is sensitive to pump-induced linear birefringence, the effect of which can be effectively eliminated by proper alignment of the actinic and probe beam polarizations. The picosecond TRCD method described here is, like conventional CD instruments, an absorptive method that is susceptible to coupling of pump-induced linear dichroism with any stray linear birefringence in the optical components before the sample. This artifact is effectively suppressed by averaging over its sinusoidal dependence on the actinic polarization angle.

An advantage of the ellipsometric method for nanosecond TRCD measurements is the lower sensitivity to instrumental noise, e.g., arc wander in xenon flash lamps. This eliminates the need for fast time modulation of the probe beam polarization, so that measurements can be extended into and beyond the time domains (milliseconds to microseconds) that correspond to cyclic periods characteristic of resonant polarization modulators used in conventional CD instruments. The price paid for this S/N amplification is the increased care required to avoid first-order linear birefringence artifacts. In the picosecond regime, the high repetition rates available for pump/probe sources make the direct absorptive measurement of CD feasible. Modulation of the probe polarization at 500 Hz is slower than the repetition rate, which allows for many pump/probe pulses per modulation cycle. The phase-sensitive detection made possible with this arrangement improves signal to noise and permits second-order pump-induced polarization artifacts to be eliminated using half-wave plate modulation.

IV. Applications

Time-resolved CD and MCD measurements have been applied to a number of systems including studies of the nature of excited states of inorganic complexes[35] and organic compounds[23d] as well as a variety of problems in biophysics.[23a–c,25b,28,32,36] Here we will discuss three examples of the applications of TRCD and TRMCD which reveal the different types of information that can be obtained from such measurements. In the first example we focus on the dynamics of the relaxation of the tertiary structure of myoglobin following photodissociation of ligated CO. The second example discusses the use of TRMCD to provide mechanistic information by probing the spin states of intermediates resulting from ligand dissociation from cytochrome *c* oxidase. Finally, TRCD spectra of primary electron transfer intermediates in the photocycle of photosynthetic bacteria demonstrate how this experimental approach can be used to study the electronic structure of biological systems.

Myoglobin. Myoglobin (Mb) is a small, 153 amino acid protein that serves as a reversible oxygen carrier within muscles of vertebrates. The structure of Mb is one of the most carefully characterized among all proteins, with refinements reported on the order of 1.5 Å.[37] Oxygen is bound and released from an iron-containing heme group which is located in the interior of the protein. The heme molecule is covalently linked to a histidine residue in the F-helix of the amino acid sequence.

Since the pioneering work by Gibson in 1956,[38] photodissociation studies of ligated myoglobin have been pursued with the goal of elucidating molecular details of the protein processes associated with ligand binding and release. In the past decade, photodissociation dynamics have been probed with a variety of time-resolved spectroscopic techniques ranging from millisecond to femtosecond resolution.[39] Relevant to the primary dissociation and relaxation processes, picosecond and femtosecond time-resolved electronic absorption spectroscopy,[40] infrared absorption spectroscopy,[41] Raman scattering,[42] various polarization spectroscopies (linear dichroism and CD),[36f,g] polarized phase gratings,[43] and hole burning[44] have been reported. Motivation for performing picosecond CD studies of ligand photodissociation can be appreciated by examining the time scales associated with the dynamics of ligand photodissociation that have been determined and those which to date have remained unanswered.

Excitation of ligated Mb generally involves promotion of a heme π electron into a π^* orbital.[45] For the Fe–ligand bond to break, this system must relax into the ligand field states. Femtosecond absorption and infrared spectroscopy clearly show that the iron–ligand bond breaks within a few hundred femtoseconds of excitation.[41] Time-resolved acoustic grating experiments show that this event is followed by a vibrational cooling of the heme; the excess heat flows into the surrounding protein with a time constant of approximately 20 ps.[44] Ligands such as NO, O_2, and isocyanide undergo considerable geminate recombination within the first few hundred picoseconds.[39] CO, on the other hand, exhibits essentially no geminate recombination on this time scale.[46] Complicated recombination dynamics are observed on longer time scales.[47] Although the above clearly shows that various important time scales are established by these techniques, two significant questions need to be directly addressed. First, what are the relaxation dynamics of the global protein structure following photodissociation? Crystallographic studies indicate several structural changes between Mb and MbCO; these global structure changes are not directly probed by the above spectroscopic studies. Second, the iron undergoes a change in spin accompanying ligation and deligation of the heme. What are the dynamics of this spin interconversion? It is expected that the time scale of this event will be a function of both bond breakage and changes in the iron–heme geometry that accompany ligand photodissociation. CD and MCD spectroscopies can provide insight into these specific questions. Before examining the results from such studies, it is instructive to consider the origin of the optical activity in Mb.

Using the three-dimensional structure of Mb from X-ray crystallographic studies, Hsu and Woody carried out theoretical calculations of CD spectra.[48] This work served to establish that the origin of the optical activity for heme transitions arose from a coupled oscillator interaction between the $\pi \rightarrow \pi^*$ transitions on the heme and those of the surrounding aromatic residues. These calculations indicated that aromatic groups as far as 12 Å away from the heme contribute appreciably to the CD spectrum. The relative orientations of those aromatic amino acids which contribute to the optical activity of the heme are shown in Figure 6. The dominant interactions are between the heme group and Phe(33,14B), Phe(43,1CD), Tyr(163,4G), and Tyr(146,23H). Although spatially close, interactions with the proximal and distal histidines, His(93,8F) and His(64,7E), respectively, are much smaller.

Considering the photodissociation process, it is reasonable to conclude that photogenerated Mb would first have the conformation of MbCO. This nonequilibrium structure must then relax to that characteristic of Mb. Based on the calculations of Hsu and Woody, dynamic evolution in tertiary structure could appear

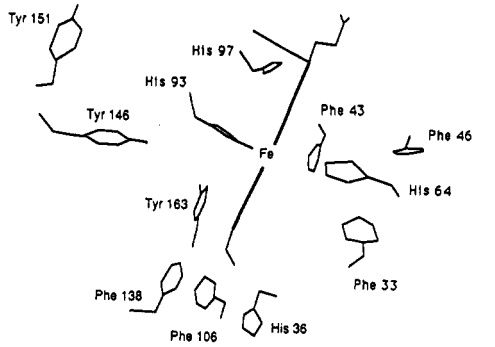

Figure 6. Orientations of the amino acids which contribute to the CD spectrum of the heme group in Mb in the UV–vis spectral range. The amino acids shown are based on reported calculations by Hsu and Woody.[48]

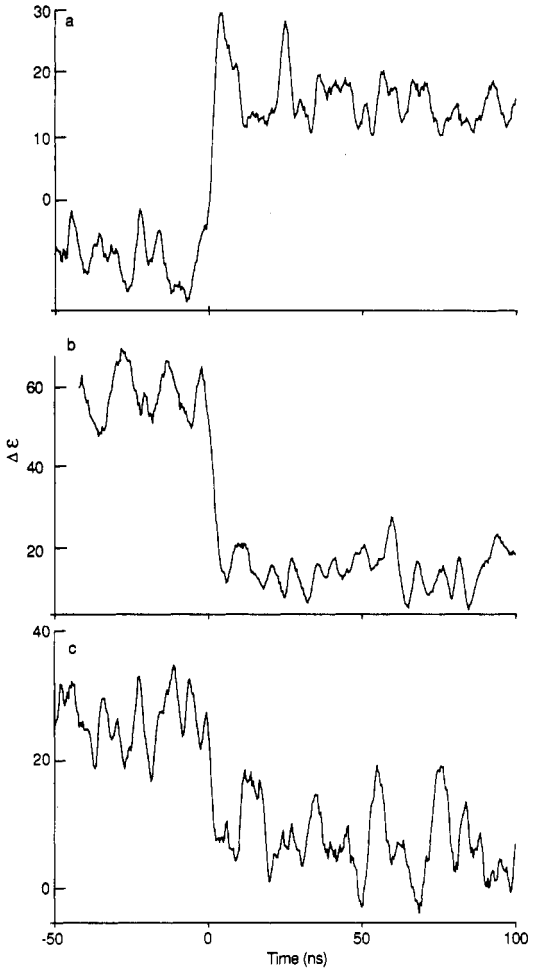

Figure 7. Nanosecond CD changes recorded for Mb following the photodissociation of CO at (a) 435, (b) 417.5, and (c) 270 nm.

as a time-dependent change in the CD signal of the heme transitions. It is important to note that even though a localized heme transition is detected, the tertiary structure of the protein is actually probed through the coupling with the aromatic residues.

The first time-resolved CD studies of the photolysis of Mb–CO were reported by Lewis et al.[23a] and Milder et al.[23c] The CD values for several absorption wavelengths changed from that expected for MbCO to that of Mb within a few nanoseconds (the resolution of the experiment); see Figure 7. No evolution in signals were observed for several hundred nanoseconds, indicating that the protein was most likely relaxing on the picosecond time scale. While it was not surprising that CD changes in the region probing heme transitions would occur within nanoseconds, these measurements provided the first demonstration that protein changes propagated from the heme region to the aromatic amino acid

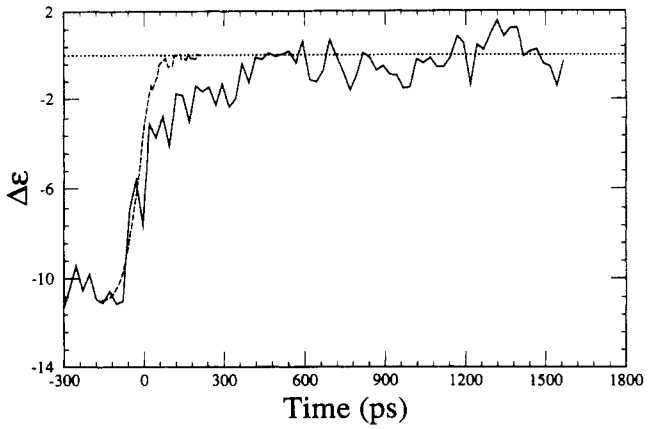

Figure 8. Transient CD kinetics of Mb probed at 355 nm following the photodissociation of CO (solid line). The dashed line is the normalized transient absorption signal recorded at this wavelength. The dotted line is the equilibrium CD value for Mb. The transient CD signal reveals two processes. The instantaneous component is due to the electronic state change that occurs upon photodissociation. The longer time signal evolution reflects conformational changes in the surrounding protein structure.

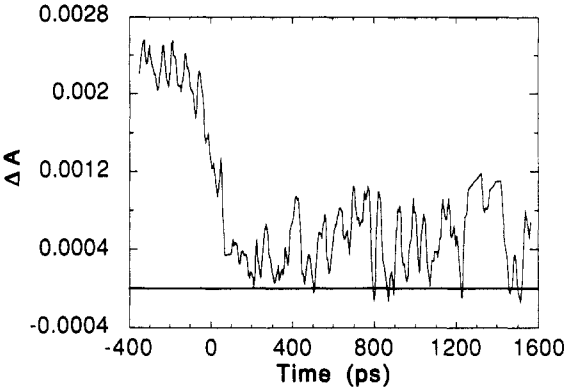

Figure 9. Transient MCD dynamics of the Q-band of Mb following picosecond photolysis of MbCO. The signal decreases to ~20% of its original value within the time resolution of the experiment. This behavior indicates that the spin state change occurs on a time scale faster than the apparatus can resolve.

regions within nanoseconds. In Figure 8, the picosecond evolution of the CD signal probed near the peak of the N-band absorption (λ = 355 nm) is plotted as a function of time following photolysis. The dashed line is a normalized transient absorption study on the same sample at the same wavelength, providing a measure of the instrument response. The CD signals observed prior to photolysis and at long times ($t > 1$ ns) are consistent with the steady-state CD values of MbCO and Mb at 355 nm, respectively. The important observation from these data is that the evolution of the CD signal is distinctly different from the transient absorption kinetics.

The picosecond CD data exhibit two major components. Approximately half of the observed signal change occurs within the instrument response. This is followed by a slower rise reflecting a relaxation process that is approximately 2 orders of magnitude slower than the dynamics of photoinduced bond cleavage (~ 200–300 fs). The instantaneous change in the CD signal following photolysis has been interpreted in terms of the electronic state change of the heme group that accompanies the change from six- to five-coordinate iron. Combined with detailed spectroscopic studies and a variety of time-resolved linear dichroism experiments, the evolution of the CD signal for several hundred picoseconds has been interpreted in terms of the relaxation of the surrounding protein structure in response to deligation.

To address the time scale on which the iron goes from low to high spin following CO elimination, picosecond MCD dynamics of the Q_0 band of Mb were examined.[28] The Q band was chosen because the MCD spectrum is very sensitive to changes in the spin state of the iron and the geometry of the heme group. In comparing Mb (high spin) to MbCO (low spin), the signal decreases by approximately a factor of 5.[49] The time-dependent MCD change at 580 nm following dissociation is shown in Figure 9. The MCD signal drops to nearly zero within the instrument response. Two important observations are obtained from these results. First, the spin-state change in Mb occurs within the time resolution of these measurements. This provides supporting evidence for the conclusion drawn from ultrafast absorption spectroscopy that the spin-state change occurs on the subpicosecond time scale. Second, within the limitations of the signal-to-noise ratio of these experiments, there is no detectable evolution of the electronic structure of the heme group from 30 ps to several nanoseconds following dissociation. This result is consistent with detailed measurements on the time evolution of the shape of the Q-band absorption.[36f]

Cytochrome *c* Oxidase. Cytochrome *c* oxidase (CcO) is the terminal oxidase in the oxidative metabolism of aerobic organisms. The resting enzyme can be reduced by accepting electrons from cytochrome *c*. In this reduced state it binds oxygen, reduces it to water, and in the process transfers protons across a cell or mitochondrial membrane.[50] Energy released by the redox chemistry powers the proton pump, and the resulting proton gradient across the membrane drives the production of ATP.

The mechanism by which CcO carries out these functions is not known, nor is detailed structural information about the protein available. Initial TRMCD studies of CcO were performed on an enzyme from bovine heart muscle, cytochrome aa_3. In this enzyme it is known that the protein contains two iron heme centers (cytochrome *a* and cytochrome a_3) with a copper atom associated with each (Cu_A and Cu_B, respectively).[51] Also present is a Zn atom and a Mg atom whose roles are not known.[52] Cytochrome *a* is a low-spin hexacoordinate heme A with two neutral histidine ligands. Cytochrome *a* and Cu_A are responsible for accepting an electron from cytochrome *c* and subsequently transferring it to the cytochrome a_3 center. Upon reduction of the a_3 center, which is a pentacoordinate high-spin heme A ligated to a histidine distal to the nearby (4–5 Å) Cu_B, cytochrome a_3 can bind another ligand to become hexacoordinate and low spin. In its normal function this sixth ligand is O_2, but as with other heme proteins, it is useful in studying this function to use CO as the sixth ligand because the Fe–CO bond is readily photodissociated with visible light.

In studying the function of CcO, the states of the enzyme following photodissociation of CO from the cytochrome a_3 center have been investigated using a number of time-resolved spectral techniques. First, time-resolved UV–vis absorption was measured on times scales from picoseconds to seconds. As with other heme proteins, absorption of light by the heme center results in dissociation of the CO ligand within femtoseconds. An increase in absorption in both the Soret (around 443 nm) and Q-band (around 610 nm) regions is then observed on a time scale of about 10 ps.[53] The resulting spectrum remains constant until a decrease in extinction (of similar magnitude to the initial increase) occurs with a half-life of about 1.5 μs. The resulting spectrum is again constant until bimolecular recombination with the CO returns the system to its initial state. This recombination occurs on a time scale of 10 ms (at a CO pressure of 1 atm). It is interesting that recombination of CO with the heme is so slow, as geminate recombination rates of CO with heme proteins typically occur in nanoseconds. Neither solvent diffusion of CO nor Fe–CO bond formation appears to be the rate-limiting step in recombination. It is also interesting that the rate of recombination is dependent on light intensity, with the rate of CO recombination accelerating with increasing light intensity incident on the sample. This is not what one might expect for recombination of a photolabile ligand.

In order to help interpret these UV–vis absorption changes, other types of time-resolved spectral techniques have been employed. Time-resolved infrared absorption showed that within picoseconds of photodissociation of CO from the Fe a Cu–CO stretching vibration at 2061 cm^{-1} appears[54] and then decays with a half-life of about 1.5 μs.[55] Initial time-resolved resonance Raman (TR^3) studies yielded spectra within 100 ns of photodissociation

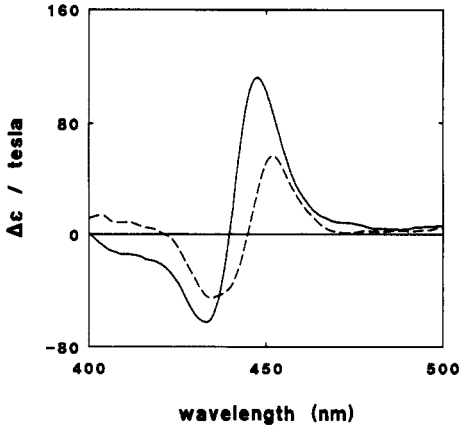

Figure 10. Soret region MCD spectra of high-spin cytochrome *c* oxidase (CcO, —) and low-spin CcO–CO (- - -).

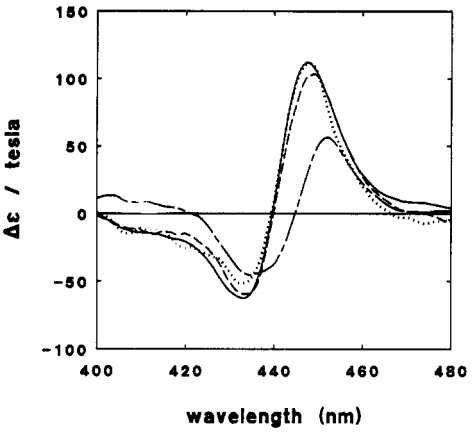

Figure 11. Nanosecond time-resolved Soret MCD spectra of CcO obtained at 100 nm (···) and 10 μs (- - -) after CO photodissociation, shown with equilibrium spectra of high-spin CcO (—) and low-spin CcO–CO (- - -).

indicative of a high-spin iron heme.[56] This would not be surprising as photodissociation would be expected to take a six-coordinate, low-spin species to a five-coordinate, high-spin species. However, since the recombination kinetics had been shown to be intensity dependent, Woodruff and co-workers measured the TR[3] spectra at greatly reduced probe laser intensity and found dramatic changes in the spectra from those obtained at high intensity.[36b] Most significantly, a band at 223 cm^{-1} became dramatically weaker in the low-intensity spectrum relative to the high-intensity spectrum 100 ns after photodissociation. This band is characteristic of an iron–histidine stretch and had been shown in studies of model compounds to be intense in high-spin hemes but weak in low-spin heme systems. These results suggested a mechanism in which photodissociation might result in a low-spin iron species persisting for times as long as microseconds. This low-spin species would be associated with a ligand shuttle between the Fe and Cu centers involving the replacement of CO by an unknown ligand after CO photodissociation to give a six-coordinate iron species.

TRMCD provides a definitive test of this model because MCD spectra are highly sensitive to the spin states of hemes. This can be seen in Figure 10 where MCD spectra in the Soret region are shown for low-spin, CO-liganded CcO as well as high-spin, unliganded CcO. These spectra show that a low-spin to high-spin transition would result in a doubling of the peak-to-trough MCD amplitudes as well as a marked blue shift in the spectrum.

In addition to the spectrum of the equilibrium low- and high-spin CcO species, Figure 11 shows MCD spectra obtained 100 ns and 10 μs after photolysis of reduced CO liganded CcO. While there are slight differences in these spectra, possibly indicating some relaxation of the heme pocket during this time, it is clear that CcO reaches a high-spin state as early as 100 ns after photolysis and that it remains high spin for some time. To get better time resolution information on the kinetics of the low-spin to

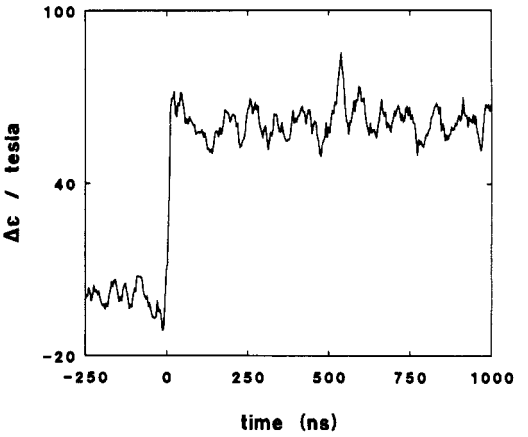

Figure 12. Nanosecond MCD signal of CcO–CO photodissociation measured at 445 nm. Risetime of photolysis signal at $t = 0$ is instrument limited.

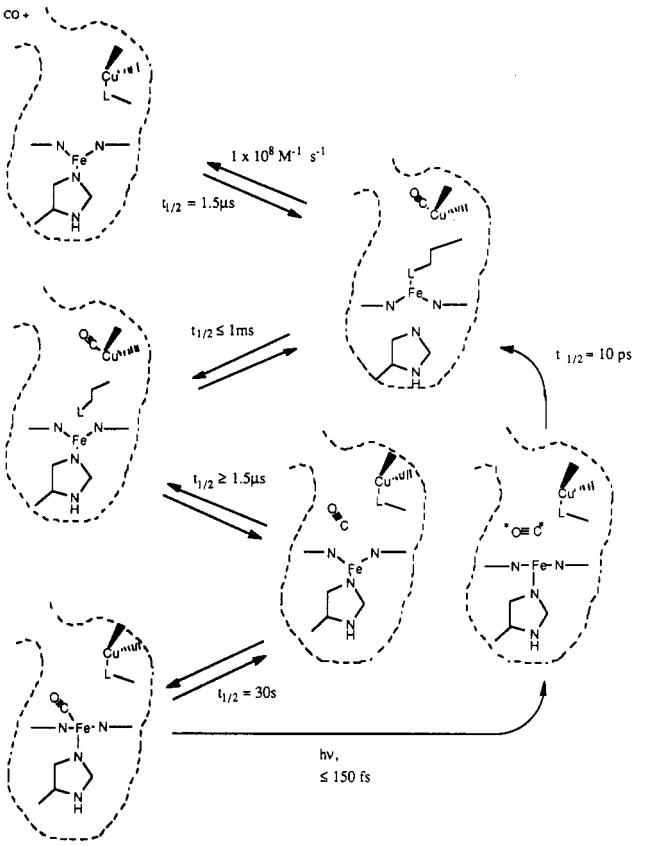

Figure 13. Schematic model of CcO–CO photodissociation and rebinding consistent with UV–vis absorption, MCD, resonance Raman, and IR time-resolved spectral evidence.

high-spin transition, MCD changes following photolysis were monitored at 445 nm. Figure 12 shows that CcO is transformed into a high-spin species within a few nanoseconds following photolysis. Longer time scale measurements showed that the CcO remains high spin until recombination with CO occurs.

Figure 13 shows a proposed mechanism for changes in CcO after photolysis as a result of these measurements. While still somewhat speculative, this mechanism explains all of the spectral observations to date. Here photolysis results in rapid dissociation of the Fe–CO bond followed by picosecond formation of a Cu–CO bond. This results in the breaking of a bond between the copper and another, as yet unidentified, ligand (L) which then forms a bond to the iron. Formation of this Fe–L bond explains the slow recombination rate of CO as the rate-limiting step for recombination would involve breaking of the Fe–L bond. It also could explain the more rapid recombination at higher light levels if the Fe–L bond were photolabile. If the Fe–L bond were to exist along

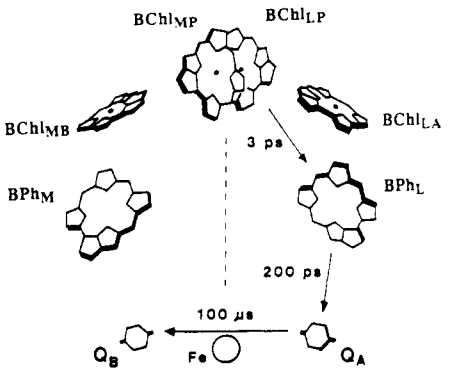

Figure 14. Spatial arrangement of the Bchls and BPhs in the RC of *Rb. sphaeroides* determined from the X-ray structure. The location of the quinones and non-heme iron are also shown. The dynamics of the electron-transfer reactions are those found at room temperature.

with the Fe–histidine bond, a long-lived low-spin species would be found. The MCD results clearly show that this is not the case. This, along with the disappearance of the Fe–histidine stretching vibration in the low-intensity Raman spectrum, leads to the conclusion that formation of the Fe–L bond results in the breaking of the Fe–histidine bond. This bond will form again and CO will recombine only after dissociation of the Fe–L bond.

This study clearly shows the value of using the TRMCD technique in conjunction with other forms of time-resolved spectroscopy. Each of the techniques used in these studies of CcO produced results which could reasonably have been interpreted by very different mechanisms. The combined information from all of the techniques, however, made it possible to restrict hypotheses about intermediates and suggest mechanisms with more confidence. Thus, the TR^3 studies and MCD studies by themselves would have reached opposite conclusions about the spin states of early intermediates. Considering data from both methods yielded a more complex and detailed mechanism.

Photosynthetic Bacteria. The primary processes of the conversion of light energy into chemical energy during photosynthesis involves the transfer of electrons between pigments embedded in a membrane protein unit commonly referred to as a reaction center (RC).[57] Recently, the three-dimensional structures of the photosynthetic RCs isolated from two bacteria, *Rhodopseudomonas viridis*[58] and *Rhodobacter sphaeroides*,[59] were reported. These results show that the RCs consist of three interacting polypeptide chains of molecular weight between 20 000 and 30 000. These chains are designated as H, L, and M, of which the H subunit is less essential to the photochemistry. The L and M subunits enclose four bacteriochlorophylls (BChl), two bacteriopheophytins (BPh), two quinones, and a non-heme iron atom. The spatial arrangement of the six molecules is shown in Figure 14. The time scales for the various electron-transfer reactions determined from transient absorption measurements are also shown.[60]

The visible and near-IR absorption spectra of the RC of *Rb. sphaeroides* at room and cryogenic temperature have been extensively studied.[61] The spectrum cannot be described as a simple sum of the absorption bands of the individual chromophores. The current view is that the electronic structure of the special pair (BChl$_{MP}$ and BChl$_{LP}$) can be described by an excitonic dimer, whereas the remaining BChls and BPhs are only subject to minor perturbations from the surrounding pigments.

In addition to studies of the optical absorption spectrum, there have been many experimental reports[62] and theoretical calculations[63] of the steady-state CD spectra. Such calculations have significantly contributed to our understanding of the electronic properties of the system. In particular, from a theoretical viewpoint, to obtain the experimental absorption and CD spectra, it is common to model the bands as corresponding to a linear combination of the eigenstates of the individual pigments. In addition, some transitions are purported to have contributions from the charge-transfer states of the dimer. For example, the low-energy exciton band of the dimer has considerable contributions from charge-transfer transitions.[63b] The CD spectra derived from such

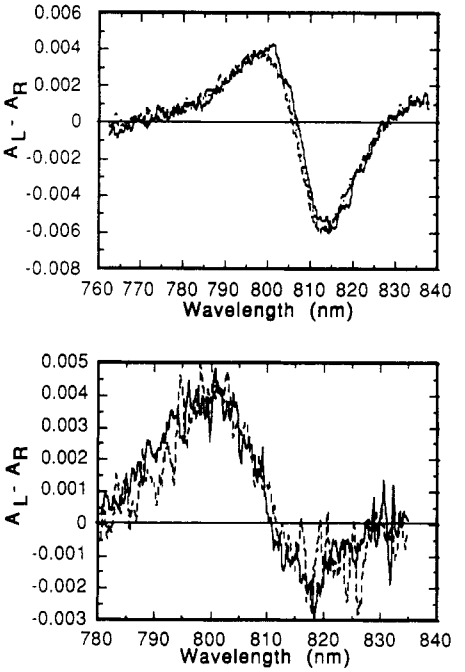

Figure 15. Near-infrared steady-state and time-resolved CD spectra. (top) Steady state near IR CD spectra of *Rb. sphaeroides* RCs with both Q_A and Q_B (—), with Q_B removed (···) and with Q_A reduced by sodium dithionite in BOG buffer (- - -) recorded by the picosecond CD spectrometer with the excitation beam blocked. The three spectra are the same, indicating that the Q_A and Q_B have a negligible effect on the CD in this spectral region. (bottom) Transient CD spectra taken at 0 (—) and 2 ns (- - -) time delay. These spectra represent the CD of the electron-transfer intermediates, $(BChl_2)^+BPh_L^-$ and $(BChl_2)^+BPh_LQ_A^-$, respectively. The incomplete vanishing of the negative CD signal at 816 nm is due to unexcited RCs (15%).

calculations have the qualitative features of experimental spectra. However, as would be expected from an excitonic theory, all these calculations predict a conservative CD spectrum (i.e., the integrated signal sums to zero), despite the fact that the experimental system has a nonconservative spectrum.[62]

In Figure 15, the steady-state CD spectrum recorded on the picosecond TRCD spectrometer (pump beam blocked) in the near-infrared region of the spectrum for RCs isolated from *Rb. sphaeroides* is shown. In addition, transient CD spectra taken at a zero (35-ps experimental resolution) and 2-ns time delay are also presented. The wavelength region probed by these experiments has been assigned to the Q_y transition of both accessory BChls. With respect to the rates of the primary electron-transfer reactions shown in Figure 14, the transient spectra shown in Figure 15 represent the CD of the following two electron-transfer intermediates, respectively: $(BChl_2)^+BPh_L^-Q_A$ and $(BChl_2)^+BPh_LQ_A^-$. Experimental measurements have confirmed that there is no evolution of the CD spectrum between 2 ns and the millisecond time scale.[27,36g]

The transient CD reveals some fascinating insights into the electronic coupling between the different pigment molecules. The data clearly show that both $(BChl_2)^+BPh_L^-Q_A$ and $(BChl_2)^+BPh_LQ_A^-$ are characterized by a large, nonexcitonic CD band at 800 nm with similar rotational strength (within 10%). In fact, the band position and rotational strength of this transient CD band are nearly identical to the corresponding band of the unexcited RCs. It is important to pay particular attention to the fact that the transient CD band remains unchanged regardless of whether the bacteriochlorophyll dimer is oxidized or the BPh_L is reduced. The radical cation of the special pair has a weak absorption band at 1250 nm,[64] and the BPh_L^- anion has an absorption between 620 and 720 nm.[57c] Both ionic intermediates should have less excitonic interactions with the two monomeric BChls than the corresponding uncharged species. In addition, if the CD band resulted from an excitonic interaction of the two monomers, the band would be conservative, in contrast to the data. Given the

near-twofold symmetry of RCs, it is hard to imagine that only excitonic interaction with BPh_M results in the 800-nm CD band. These observations cast serious doubts on an excitonic origin of this CD band.

These time-resolved CD measurements suggest that, contrary to current models, mechanisms other than exciton interaction need to be considered in accounting for the CD of the bacteriochlorophyll monomer transition at 800 nm. Various hypotheses can be proposed which can account for the experimental observations. First, the monomer BCls could be intrinsically chiral, perhaps arising from structural properties such as a doming of the porphyrin due to the five-coordinated Mg or the nonplanarity of the porphyrin side chains. Second, coupled oscillator interaction between $\pi \rightarrow \pi^*$ transitions on the prosthetic groups and the aromatic side chains of the protein can also contribute significantly to CD spectra, as can be seen in the case of Mb.[48] In the RC, there are numerous phenylalanine, tyrosine, and tryptophan residues in close proximity to the pigments. Interactions with these groups could result in substantial contributions to the CD signal. Further experiments are needed to understand the observed results; however, this study demonstrates that TRCD is a useful probe of electronic structure in biological systems.

V. Future Directions

This article has focused on recent developments which enable the collection of transient nanosecond and picosecond CD spectra in the visible and near-infrared spectral region. While this spectral range allows for the study of many important biological processes, extensions of these techniques into the ultraviolet region would represent a significant advance. In the UV, the CD spectrum results from the secondary structure of the amino acids in proteins.[65] The development of time-resolved CD techniques in the UV would allow for the study the conformation dynamics of biological molecules that do not contain visible light absorbing chromophores. Helix–coil transitions on the time scales associated with the primary steps of protein folding and unfolding and conformation changes in DNA following excitation of intercalated molecules are only two of the biological problems that could be addressed by such technology.

In the past year, the collection of transient infrared spectra with subpicosecond resolution has become possible.[66] This technical advance provides the possibility of carrying out transient vibrational circular dichroism (VCD) measurements on ultrafast time scales. At present, the signal-to-noise ratios in the transient absorption experiments are not sufficient for measuring VCD signals. However, it is likely that future advances in infrared laser systems and associated detection electronics will result in capabilities similar to the visible techniques that exist today. Recent studies suggest that VCD spectra are more simply related to protein secondary structure than UVCD spectra.[67] Thus, in the long term, development of transient VCD spectroscopy may represent a significant advance in quantifying the time scales of motions in biological systems.

Accompanying the advances in experimental techniques, new theoretical methods for calculating the effects of conformational motions on CD spectra are required. In the past few years, many advances have been made in calculating the time evolution of spectroscopic properties of molecules. In the case of photodissociation reactions of small molecules, excellent agreement between the experimental and calculated time evolutions of optical spectra has been reported.[68] Further developments in theoretical techniques for calculating optical properties of molecular systems could enable the direct connection between specific molecular motions and the time evolution of CD signals.

Acknowledgment. This work is supported by grants from the National Science Foundation (J.D.S., CHE-90-13138), National Institutes of Health (J.D.S., GM-49142; D.S.K., GM-35158 and GM-38549) and the MMFEL program administered by the Office of Naval Research (J.D.S.). We thank our co-workers over the past several years who have contributed to the work described in this paper: Sofie Björling, Ólöf Einarsdóttir, George Feher, Tack Kuntz, Steve Milder, Mel Okamura, Cora Einterz Randall, and Woody Woodruff.

References and Notes

(1) Schoenlein, R. W.; Peteanu, L. A.; Mathies, R. A.; Shank, C. V. *Science* **1991**, *254*, 412.
(2) (a) Mathies, R. A.; Cruz, C. H. B.; Pollard, W. T.; Shank, C. V. *Science* **1988**, *240*, 777. (b) Mathies, R. A.; Lin, S. W.; Ames, J. B.; Pollard, W. T. *Annu. Rev. Biophys. Biophys. Chem.* **1991**, *20*, 491.
(3) Karplus, M.; McCammon, J. A. *Nature* **1979**, *227*, 578.
(4) (a) Murray, L. P.; Hofrichter, J.; Henry, E. R.; Eaton, W. A. *Biophys. Chem.* **1988**, *90*, 63. (b) Birge, R. R. *Biochim. Biophys. Acta* **1990**, *293*, 1016.
(5) (a) Hofrichter, J.; Sommer, J. H.; Henry, E. R.; Eaton, W. A. *Proc. Natl. Acad. Sci. U.S.A.* **1983**, *80*, 2235. (b) Spiro, T. G.; Smuleviich, G.; Su, Chang *Biochemistry* **1990**, *19*, 4497. (c) Perutz, M. *Mechanisms of Cooperativity and Allosteric Regulation in Proteins*; Cambridge University Press: Cambridge, 1990. (d) Sawicki, C. A.; Gibson, Q. H. *J. Biol. Chem.* **1976**, *251*, 1533.
(6) (a) Campbell, I. D.; Dobson, C. H.; Williams, R. J. P. *Adv. Chem. Phys.* **1978**, *39*, 35. (b) Wagner, G.; Wuthreih, K. *Methods Enzymol.* **1986**, *131*, 307.
(7) Simon, J. D. *Rev. Sci. Instrum.* **1989**, *60*, 3597.
(8) Weber, G. In *Advances in Protein Chemistry*; Anson, M. L., Bailey, K., Edsall, J. T., Eds.; Academic Press: New York, 1953.
(9) (a) Maliwal, B. P.; Lakowicz, J. R. *Biophys. Chem.* **1984**, *19*, 337. (b) Beecham, J. M.; Brand, L. *Annu. Rev. Biochem.* **1985**, *54*, 43. (c) Cross, A. J.; Fleming, G. R. *J. Biophys.* **1986**, *50*, 507 and references cited therein.
(10) (a) Eaton, W. A.; Hofrichter, J. *Methods Enzymol.* **1981**, *76*, 175.
(11) (a) Lakowicz, J. R., Ed. *Time-Resolved Laser Spectroscopy in Biochemistry II*; *Proc. SPIE* **1990**, 1204. (b) Lakowicz, J. R., Ed. *Time-Resolved Laser Spectroscopy in Biochemistry III*; *Proc. SPIE*, in press. (c) Birge, R. R.; Nafie, L. A. *Biomolecular Spectroscopy II*; *Proc. SPIE* **1990**, 1432.
(12) (a) Creighton, T. E. *Proteins*; W. H. Freeman: New York, 1984. (b) Cantor, C. R.; Schimmel, P. R. *Biophysical Chemistry*; W.H. Freeman: New York, 1980. (c) Johnson, W. C.; Tinoco, I. *J. Am. Chem. Soc.* **1972**, *94*, 4389. (d) Greenfield, N.; Fasman, C. D. *Biochemistry* **1969**, *8*, 4108 and references cited therein.
(13) Circular dichroism is also frequently reported as ellipticity, [Θ]. [Θ] and $\Delta\epsilon$ are related by $[\Theta] = 3300\Delta\epsilon$.
(14) (a) Lowry, R. *Optical Rotatory Power*; Longmans Green and Co.: London, 1935. (b) Cotton, A. *C. R. Acad. Sci.* **1895**, *120*, 989.
(15) Haidinger, W. *Poggendorf's Ann.* **1847**, *70*, 531.
(16) Mitchell, S. *J. Chem. Soc.* **1928**, 3258.
(17) Velluz, L.; Legrand, M.; Grosjean, M. *Optical Circular Dichroism*; Academic Press: New York, 1965.
(18) Billardon, M.; Badoz, J. *C. R. Acad. Sci.* **1966**, *262*, 1672.
(19) Applequist, J. *Am. Sci.* **1987**, *75*, 59.
(20) (a) Bayley, P. M.; Anson, M. *Biopolymers* **1974**, *13*, 401. (b) Luchias, J.; Beychok, S. *Science* **1978**, *199*, 425.
(21) (a) Bayley, P.; Martin, S.; Anson, M. *Biochem. Biophys. Res. Commun.* **1975**, *66*, 303. (b) Anson, M.; Martin, S. R.; Bayley, P. *Rev. Sci. Instrum.* **1977**, *48*, 953. (c) Gruenewald, B.; Knoche, W. *Rev. Sci. Instrum.* **1978**, *49*, 797. (d) Ferrone, F. A.; Hopfield, J. J.; Schatterly, S. E. *Rev. Sci. Instrum.* **1974**, *45*, 1392.
(22) Metcalf, D. H.; Snyder, S. W.; Wu, S.; Hilmes, G. J.; Richl, J. P.; Demas, J. N.; Richardson, F. S. *J. Am. Chem. Soc.* **1989**, *111*, 3082.
(23) (a) Lewis, J. W.; Tilton, R. F.; Einterz, C. M.; Milder, S. J.; Kuntz, I. D.; Kliger, D. S. *J. Phys. Chem.* **1985**, *89*, 289. (b) Einterz, C. M.; Lewis, J. W.; Milder, S. J.; Kliger, D. S. *J. Phys. Chem.* **1985**, *89*, 3845. (c) Milder, S. J.; Björling, S. C.; Kuntz, I. D.; Kliger, D. S. *Biophys. J.* **1988**, *53*, 659. (d) Kliger, D. S.; Lewis, J. W. *Rev. Chem. Intermed.* **1987**, *8*, 367. (e) Goldbeck, R. A.; Dawes, T. D.; Milder, S. J.; Lewis, J. W.; Kliger, D. S. *Chem. Phys. Lett.* **1989**, *156*, 545.
(24) (a) Xie, X.; Simon, J. D. *Opt. Commun.* **1989**, *69*, 303. (b) In previous reports, the oscillator has also been cavity dumped to provide high-energy pulses at 532, 355, and 266 nm, which can be used for excitation.
(25) (a) Xie, X.; Simon, J. D. *Rev. Sci. Instrum.* **1989**, *60*, 2614. (b) Xie, X.; Simon, J. D. *Proc. SPIE* **1990**, *1204*, 66.
(26) Xie, X.; Simon, J. D. *J. Opt. Soc. Am. B* **1990**, *7*, 1673.
(27) Xie, X.; Simon, J. D. *Biochim. Biophys. Acta* **1991**, *1057*, 131.
(28) Xie, X.; Simon, J. D. *J. Phys. Chem.* **1990**, *94*, 8014.
(29) It should be pointed out that it is possible to cancel the effect of CB in a null ($\xi = 0$) CD measurement if an analyzing quarter-wave plate is used to convert the induced ellipticity to a rotation, the sign of which will depend on the sign of the CD and the quarter-wave plate orientation. Reversing the orientation of the quarter-wave plate reverses the rotation due to CD but not CB, allowing the latter to be canceled. This method predates the use of photoelectric detection, when rotation was measured by turning the analyzing polarizer and nulling transmission by eye.
(30) This comparison assumes that f is constant between methods, which may not be the case if different sampling frequencies are used. For a differential method, instrumental noise as defined here is essentially the time derivative of intensity integrated over the sampling period (more precisely, the standard deviation of the distribution of these values). Thus, f will roll off at high frequencies for noise sources such as arc wander. In particular, different f values would be required to compare the ellipsometric apparatus described here with a conventional CD instrument, even assuming identical light sources. The latter instrument uses a lock-in amplifier paired with high-frequency modulation to select a sampling frequency where f is small

enough to achieve the S/N needed for CD detection.

(31) Moscowitz, A. *Adv. Chem. Phys.* **1962**, *4*, 67.

(32) Björling, S. C.; Goldbeck, R. A.; Milder, S. J.; Randall, C. E.; Lewis, J. W.; Kliger, D. S. *J. Phys. Chem.* **1991**, *95*, 4685.

(33) Einterz, C. M.; Lewis, J. W.; Milder, S. J.; Kliger, D. S. *J. Phys. Chem.* **1985**, *89*, 3845.

(34) To the extent that anisotropy is introduced into the intensity detection, e.g., through polarization bias in gratings or photodetectors, stray and pump-induced LB artifacts can also appear in an absorptive CD measurement.

(35) (a) Gold, J. S.; Milder, S. J.; Lewis, J. W.; Kliger, D. S. *J. Am. Chem. Soc.* **1985**, *107*, 8285. (b) Milder, S. J.; Gold, J. S.; Kliger, D. S. *J. Am. Chem. Soc.* **1986**, *108*, 8295. (c) Milder, S. J.; Gold, J. S.; Kliger, D. S. *Chem. Phys. Lett.* **1988**, *144*, 269. (d) Milder, S. J.; Gold, J. S.; Kliger, D. S. *Inorg. Chem.* **1990**, *29*, 2506.

(36) (a) Milder, S. J.; Weiss, P. S.; Kliger, D. S. *Biochemistry* **1989**, *28*, 2258. (b) Woodruff, W. H.; Einarsdottir, O.; Dyer, R. B.; Bagley, K. A.; Palmer, G.; Atherton, S. J.; Goldbeck, R. A.; Dawes, T. D.; Kliger, D. S. *Proc. Natl. Acad. Sci. U.S.A.* **1991**, *88*, 2588. (c) Goldbeck, R. A.; Dawes, T. D.; Einarsdottir, O.; Woodruff, W. H.; Kliger, D. S. *Biophys. J.* **1991**, *60*, 125. (d) Goldbeck, R. A.; Björling, S. C.; Kliger, D. S. *Proc. SPIE* **1991**, *1432*, 14. (e) Xie, X.; Simon, J. D. *J. Am. Chem. Soc.* **1990**, *112*, 7802. (f) Xie, X.; Simon, J. D. *Biochemistry* **1991**, *30*, 3682. (g) Simon, J. D.; Xie, X.; Dunn, R. C. *Proc. SPIE* **1991**, *1432*, 211.

(37) Kuriyan, J.; Wilz, S.; Karplus, M.; Petsko, G. A. *J. Mol. Biol.* **1986**, *192*, 133.

(38) Gibson, Q. H. *J. Physiol.* **1956**, *136*, 112.

(39) Hochstrasser, R. M.; Johnson, C. K. In *Ultrashort Laser Pulses and Applications, Topics in Applied Physics*; Kaiser, W., Ed.; Springer-Verlag: New York, 1988; Vol. 60.

(40) (a) Greene, B. I.; Hochstrasser, R. M.; Weisman, R. B.; Eaton, W. A. *Proc. Natl. Acad. Sci. U.S.A.* **1978**, *75*, 5255. (b) Jongeward, K. A.; Magde, D.; Taube, D. J.; Marsters, J.; Traylor, T. *J. Am. Chem. Soc.* **1988**, *110*, 380. (c) Martin, J. L.; Migus, A.; Poyart, C.; Lecarpentier, Y.; Astier, R.; Antonetti, A. *Proc. Natl. Acad. Sci. U.S.A.* **1983**, *80*, 173. (d) Lambright, D. G.; Balasubramanian, S.; Boxer, S. G. *Chem. Phys.* **1991**, *158*, 249.

(41) (a) Anfinrud, P. A.; Han, C.; Hochstrasser, R. M. *Proc. Natl. Acad. Sci. U.S.A.* **1989**, *86*, 8387. (b) Moore, J. N.; Hansen, P. A.; Hochstrasser, R. M. *Proc. Natl. Acad. Sci. U.S.A.* **1988**, *85*, 5062. (c) Lock, B.; Lian, T.; Hochstrasser, R. M. *Chem. Phys.* **1991**, *158*, 409.

(42) (a) Dasgupta, S.; Spiro, T. G.; Johnson, C. K.; Daliskas, G. A.; Hochstrasser, R. M. *Biochemistry* **1985**, *24*, 5295. (b) Findsen, E. W.; Scott, T. W.; Chance, M. R.; Friedman, J. M. *J. Am. Chem. Soc.* **1985**, *107*, 3355. (c) Petrich, J. W.; Martin, J. L.; Houde, D.; Orszaq, A. *Biochemistry* **1987**, *26*, 7914. (d) Terner, J.; Spiro, T. G.; Nagumo, M.; Nicol, M. F.; El-Sayed, M. A. *J. Am. Chem. Soc.* **1980**, *102*, 3238. (e) Lingle, R.; Xu, X.; Zhu, H.; Yu, S.; Hopkins, J. B. *J. Am. Chem. Soc.* **1991**, *113*, 3992.

(43) (a) Genberg, L.; Heisel, F.; McLenson, G.; Miller, R. J. D. *J. Phys. Chem.* **1987**, *91*, 5521. (b) Genberg, L.; Bao, Q.; Gracewskiz, S.; Miller, R. J. D. *Chem. Phys.* **1989**, *31*, 31. (c) Genberg, L.; Richard, L.; McLendon, G.; Miller, R. J. D. *Science* **1991**, *251*, 1051.

(44) Campbell, B. F.; Chance, M. R.; Friedman, J. M. *Science* **1987**, *238*, 373.

(45) (a) Gouterman, M. *J. Mol. Spectrosc.* **1961**, *6*, 138. (b) Gouterman, M. In *The Porphyrins*; Dolphin, D., Ed.; Academic Press: New York, 1978; Vol. III. (c) Eaton, W. A.; Hofrichter, J. *Methods Enzymol.* **1981**, *76*, 175. (d) Iizuka, T.; Yamamoto, H.; Kontani, M.; Yonetani, T. *Biochim. Biophys. Acta* **1974**, *371*, 126.

(46) (a) Henry, E. R.; Sommer, J. H.; Hofrichter, J.; Eaton, W. A. *J. Mol. Biol.* **1983**, *166*, 443. (b) Henry, E. R.; Eaton, W. A.; Hochstrasser, R. M. *Proc. Natl. Acad. Sci. U.S.A.* **1986**, *83*, 8982.

(47) (a) Frauenfelder, H.; Alberding, N. A.; Ansari, A.; Braunstein, D.; Cowen, B. R.; Hong, M. K.; Iben, I. E. T.; Johnson, J. B.; Luck, S.; Marden, M. C.; Mourant, J. R.; Ormos, P.; Reinisch, L.; Scholl, R.; Schulte, A.; Shyamsunder, E.; Sorensen, L. B.; Steinback, P.; Xie, A.; Young, R. D.; Lee, K. T. *J. Phys. Chem.* **1990**, *94*, 1024. (b) Friedman, J. M.; Lyons, K. B. *Nature* **1980**, *284*, 570. (c) Alpert, B.; ElMohsni, S.; Lindqvist, L.; Tfibel, F. *Chem. Phys. Lett.* **1979**, *64*, 111. (d) Chernoff, D. A.; Hochstrasser, R. M.; Steel, A. W. *Proc. Natl. Acad. Sci. U.S.A.* **1980**, *77*, 5606. (e) Duddell, D. A.; Morris, R. J.; Richards, J. T. *J. Chem. Soc., Chem. Commun.* **1979**, 75. (f) Young, R. D.; Frauenfelder, H.; Johnson, J. B.; Lamb, D. C.; Nienhaus, G. U.; Philipp, R.; Scholl, R. *Chem. Phys.* **1991**, *158*, 315.

(48) (a) Hsu, M.-C.; Woody, R. W. *J. Am. Chem. Soc.* **1971**, *93*, 3515. (b) Hsu, M.-C.; Woody, R. W. *J. Am. Chem. Soc.* **1969**, *91*, 3679. (c) Woody, R. In *Biochemical and Clinical Aspects of Hemoglobin Abnormalities*; Academic Press: New York, 1978.

(49) (a) Springall, J.; Stillman, M. J.; Thomson, A. J. *Biochim. Biophys. Acta* **1976**, *453*, 494. (b) Bolard, J.; Garnier, A. *Biochim. Biophys. Acta* **1972**, *263*, 535. (c) Kajiyoshi, M.; Anon, F. K. *J. Biochem.* **1975**, 1087. (d) Holmquit, B. In *The Porphyrins*; Dolphin, D., Ed.; Academic Press: New York, 1978; Vol. III. (e) Sutherland, J. C. In *The Porphyrins*; Dolphin, D., Ed.; Academic Press: New York, 1978; Vol. III.

(50) Chan, S. I.; Li, P. M. *Biochemistry* **1990**, *29*, 1.

(51) (a) Wikstrom, M.; Saraste, M.; Penttila, T. In *The Enzymes of Biological Membranes, Vol. 4, Bioenergetics of Electron and Proton Transport*; Martonosi, A. N., Ed.; Plenum: New York, 1985. (b) Scott, R. A. *Annu. Rev. Biophys. Biophys. Chem.* **1989**, *18*, 137.

(52) Einarsdottir, O.; Caughey, W. S. *Biochem. Biophys. Res. Commun.* **1985**, *129*, 840.

(53) Einarsdottir, O.; Killough, P. M.; Dyer, R. B.; Lopez-Garriga, J. J.; Hubig, S. M.; Atherton, S. J.; Palmer, G.; Woodruff, W. H. To be published.

(54) Dyer, R. B.; Peterson, K. A.; Stoutland, P. O.; Woodruff, W. H. *J. Am. Chem. Soc.* **1991**, *113*, 6276.

(55) Dyer, R. B.; Einarsdottir, O.; Killough, P. M.; Lopez-Garriga, J. J.; Woodruff, W. H. *J. Am. Chem. Soc.* **1989**, *111*, 7657.

(56) Findsen, E. W.; Centeno, J.; Babcock, G. T.; Ondrias, M. R. *J. Am. Chem. Soc.* **1987**, *109*, 5367.

(57) (a) Feher, G.; Allen, J. P.; Okamura, M. Y.; Rees, D. C. *Nature* **1989**, *339*, 111. (b) Friesner, R. A.; Won, Y. *Biochim. Biophys. Acta* **1989**, *977*, 99. (c) Kirmaier, C.; Holten, D. *Photosynth. Res.* **1987**, *13*, 225.

(58) Deisenhofer, J.; Epp, O.; Miki, R.; Huber, R.; Michel, H. *Nature* **1985**, *318*, 618.

(59) (a) Allen, J. P.; Feher, G.; Komiya, T. O.; Rees, D. C. *Proc. Natl. Acad. Sci. U.S.A.* **1988**, *85*, 8487. (b) Chang, C.-H.; Tiede, D.; Tang, J.; Smith, U.; Norris, J. R.; Schiffer, M. *FEBS Lett.* **1986**, *205*, 82.

(60) (a) Breton, J.; Martin, J. L.; Migus, A.; Antonetti, A.; Orszag, A. *Proc. Natl. Acad. Sci. U.S.A.* **1986**, *83*, 5121. (b) Martin, J. L.; Breton, J.; Hoff, A. J.; Migus, A.; Antonetti, A. *Proc. Natl. Acad. Sci. U.S.A.* **1986**, *83*, 957. (c) Fleming, G. R.; Martin, J. L.; Breton, J. *Nature* **1988**, *333*, 190. (d) Holzapfel, W.; Finkele, U.; Kaiser, W.; Oesterhett, D.; Scheer, H.; Stilz, H. U.; Zinth, W. *Chem. Phys. Lett.* **1989**, *160*, 1. (e) Vos, M. H.; Lambry, J.-C.; Robles, S. J.; Youvan, D. C.; Breton, J.; Martin, J.-L. *Proc. Natl. Acad. Sci. U.S.A.* **1991**, *88*, 8885. (f) Kirmaier, C.; Holton, D.; Parson, W. W. *Biochim. Biophys. Acta* **1985**, *810*, 49. (g) Kirmaier, C.; Holton, D.; Bylina, E. J.; Youvan, D. C. *Proc. Natl. Acad. Sci. U.S.A.* **1988**, *85*, 7562.

(61) (a) Breton, J.; Vermeglio, A. In *Photosynthesis, Vol. 1: Energy Conversion by Plants and Bacteria*; Govindjee, Ed.,; Academic Press: New York, 1982. (b) Paillotin, G.; Vermeglio, A.; Breton, J. *Biochim. Biophys. Acta* **1979**, *545*, 249.

(62) (a) Schuvalov, V. A.; Asadov, A. A. *Biochim. Biophys. Acta* **1979**, *545*, 296. (b) Mar, T.; Gingras, G. *Biochim. Biophys. Acta* **1984**, *764*, 283. (c) Philipson, K. D.; Sauer, K. *Biochemistry* **1973**, *12*, 535. (d) Reed, D. W.; Ke, B. *J. Biol. Chem.* **1972**, *248*, 3041. (e) Breton, J. *Biochim. Biophys. Acta* **1985**, *810*, 235.

(63) (a) Won, Y.; Friesner, R. A. *J. Phys. Chem.* **1988**, *92*, 2208. (b) Warshel, A.; Parson, W. W. *J. Am. Chem. Soc.* **1987**, *109*, 6143. (c) Parson, W. W.; Warshel, A. *J. Am. Chem. Soc.* **1987**, *109*, 6152. (d) Knapp, E. W.; Fischer, S. F.; Zinth, W.; Sander, M.; Kaiser, W.; Deisenhofer, J.; Michel, H. *Proc. Natl. Acad. Sci. U.S.A.* **1985**, *82*, 8463. (e) Knapp, E. W.; Scherer, P. O. J.; Fisher, S. F. *Biochim. Biophys. Acta* **1986**, *852*, 295.

(64) Feher, G. *Photochem. Photobiol.* **1971**, *14*, 373.

(65) Stryer, L. *Biochemistry*; Freeman: New York, 1981.

(66) Locke, B.; Lian, T.; Hochstrasser, R. M. *Chem. Phys.* **1991**, *158*, 409.

(67) (a) Pancoska, P.; Keiderling, T. A. *Biochemistry* **1991**, *30*, 6885. (b) Pancoska, P.; Yasui, S. C.; Keiderling, T. A. *Biochemistry* **1991**, *30*, 5089.

(68) Khundar, L.; Zewail, A. H. *Annu. Rev. Phys. Chem.* **1990**, *41*, 15.